J. exp. Biol. **130**, 87–106 (1987)
Printed in Great Britain © *The Company of Biologists Limited 1987*

ARTERIAL HAEMODYNAMICS IN THE CEPHALOPOD MOLLUSC, *OCTOPUS DOFLEINI*

BY ROBERT E. SHADWICK*, JOHN M. GOSLINE AND WILLIAM K. MILSOM

Department of Zoology, University of British Columbia, Vancouver, BC Canada

Accepted 24 March 1987

SUMMARY

Simultaneous measurements of blood pressure and blood flow were made in the dorsal aorta of the cephalopod *Octopus dofleini* Wülker. In resting animals the heart rate varied from 8·5 to 14 beats min^{-1}, while aortic pressure typically ranged from about 2·5 kPa at end diastole to 5·5 kPa at peak systole. Blood flow rate varied with pressure, averaging 0·9 ml s^{-1}, with peak flow rates of 1·4–2·8 ml s^{-1}. A slow asymptotic decline in both pressure and flow during the 2- to 4-s diastolic period indicated that the aorta functions as an elastic reservoir, as previously predicted. Aortic impedance spectra were derived from digitized pressure and flow data. The impedance amplitude decreased continuously with increasing frequency, while the impedance phase was always negative. These results are consistent with a two-element Windkessel model of the arterial system. The apparent pressure wave velocity, determined from transit times of pressure pulses *in vivo*, was >10 m s^{-1}. This was much higher than the intrinsic wave velocity we predicted from *in vitro* measurements of aortic elasticity. This anomaly occurred because the length of the aorta represented less than 1% of the wavelength of the fundamental pulse frequency, due to the low heart rate in this species. Consequently, arterial haemodynamics in *O. dofleini* are dominated by strong wave reflections, but do not exhibit other wave propagation effects which are typical of mammalian circulatory systems. Thus, the simple Windkessel model adequately describes the arterial circulation of this species of cephalopod.

INTRODUCTION

The circulatory system in cephalopod molluscs is remarkably different from the low-pressure, open vascular systems which are typical of other invertebrates. In cephalopods, blood circulation is through a well-developed, closed network of vessels which in many ways parallels the circulatory systems of lower vertebrates (Packard, 1972). Previous studies on octopuses indicate that these cephalopods have a relatively high-pressure arterial system (Johansen & Martin, 1962; Wells, 1979), but little is known about the mechanics of blood flow in these advanced invertebrates. Recently,

* Present address: Department of Biology, University of Calgary, Calgary, Alberta, Canada T2N 1N4.

Key words: octopus, haemodynamics, vascular impedance, pressure wave velocity, Windkessel.

we investigated the mechanical properties of the dorsal aorta of *Octopus dofleini in vitro* and found that this vessel is a highly extensible and resilient elastic tube, much like the arteries of vertebrates (Shadwick & Gosline, 1985). We suggested that the aorta should function *in vivo* as an effective elastic reservoir, and the present study demonstrates that this is indeed the case.

In a simple model the major arteries are considered to function as a single elastic chamber, or 'Windkessel', while the peripheral vessels are represented by a single non-compliant resistance element (Fig. 1). The elastic chamber is distended with blood during systolic ejection from the heart, and discharges blood through the resistance by passive elastic recoil in diastole. Thus, intermittent output from the heart is transformed by the elasticity of the chamber into a relatively steady flow to the periphery. The importance of this pulse-smoothing effect by the large arteries in the mammalian circulation has been recognized since the eighteenth century (see McDonald, 1974). The Windkessel model assumes that there is a distinct division between capacitive and resistive portions of the arterial tree, and that pressure changes occur simultaneously throughout the system, i.e. the pressure pulse is transmitted at infinite velocity.

The major fault of the Windkessel model, in application to mammalian circulation, is that it makes no allowance for wave propagation effects which result from finite transmission times (Taylor, 1964): when arterial pressure waves are propagated over

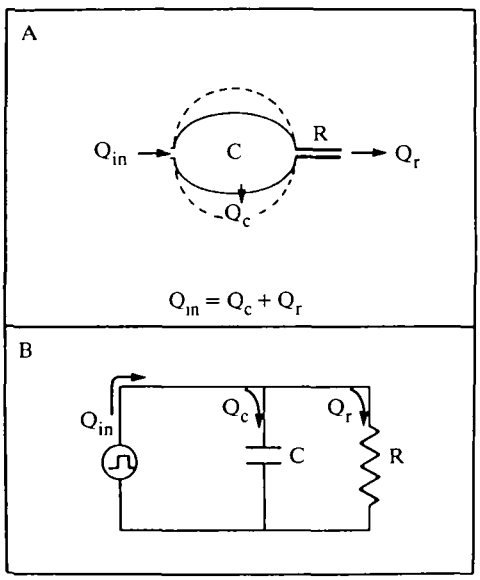

Fig. 1. (A) A Windkessel model of the circulation. The major arteries are represented by a single elastic chamber with compliance C, while the peripheral vasculature is represented by a single resistance R. The total flow into the system, Q_{in}, is the sum of the volume change of the elastic chamber, Q_c, and the simultaneous flow across R, Q_r. (B) An electrical analogue of the Windkessel model. A capacitor represents the elastic chamber, while a resistor represents the peripheral resistance. The total current flow in this circuit, Q_{in}, is equal to the flow through C, Q_c, plus the flow through R, Q_r.

distances which approach or exceed their wavelengths, as is the case in mammals (Noordergraaf, Li & Campbell, 1979), the system does not behave like a simple elastic reservoir. Rather, the mammalian arterial tree is better described by transmission line theories which incorporate phenomena such as amplification and distortion of the travelling pressure wave, frequency-dependent oscillations in the impedance and apparent wave velocity, distributed reflection sites, and 'elastic taper' (Taylor, 1964, 1965).

It has been shown that arterial haemodynamic relationships in small poikilothermic vertebrates, such as turtles and frogs, can be described by Windkessel models (Burggren, 1977; Langille & Jones, 1977). The important difference between these animals and mammals is that, for comparable size, the resting heart rate in poikilotherms is considerably lower. Thus, the transmission time of the pressure pulse through the arterial circulation becomes a negligible proportion of the cardiac cycle, and therefore complex wave propagation theories are not necessary to model the dynamics of blood flow in these animals. The purpose of the present study was to make simultaneous measurements of aortic blood pressure and flow in the octopus, and to assess the role of the aorta as a simple Windkessel in this cephalopod.

METHODS AND THEORETICAL BACKGROUND

Measurements of arterial blood pressure and flow

Experiments were performed on five healthy specimens of *O. dofleini* which weighed between 8 and 11 kg. The animals were anaesthetized by chilling, or by exposure to 2 % ethanol in sea water. A mid-line incision was made through the skin and dorsal mantle wall (see Wells, 1983, for details of the anatomy). The dorsal aorta, the major artery from the systemic heart, was exposed by carefully opening the underlying body wall. It was not possible to reach the aortic root without rupturing a large venous sinus, so for cannulation the vessel was sectioned about 5 cm from the heart and rejoined by a short T-piece of vinyl tubing. The operation usually took less than 10 min, and blood loss appeared to be very slight. In each case, the diameter of the tubing was selected to match the anticipated aortic diameter at resting diastolic pressure. Two identical lengths of PE 90 tubing were introduced into the aorta *via* the side-arm of the T-piece; one was advanced a measured distance from the other. The arm of the T-piece was sealed over with cyanoacrylate glue, allowing the catheter to emerge with no blood leakage. The catheters were filled with filtered sea water and connected to identical Bio-tec BT 70 pressure transducers. The vinyl T-piece also contained a blood flow probe from a Biotronix BL 610 electromagnetic flowmeter, and a pneumatic flow occluder which was used to establish zero flow. The total length of the T-piece including flow probe was 16 mm. Immediately after surgery, the animal was revived in an aquarium filled with aerated sea water at 8–10 °C. Provided that the sensitive outer skin was not stitched (suggested by Wells, 1979), the animals were not irritated by the presence of the catheters. Recording

sessions were successfully carried out over periods of several hours on unrestrained, unanaesthetized animals. To achieve reasonable measurements of the 'resting' state, the animals were maintained undisturbed under low light levels in covered aquaria.

The pressure transducers were calibrated statically against columns of sea water, and dynamically by monitoring the free vibrations from a pressure transient applied at the catheter tips. The resonant frequency of the pressure recording system was always over 40 Hz. Since this was about 40 times greater than the highest relevant frequencies recorded in these experiments, no phase or amplitude corrections to the pressure signals were necessary. The electromagnetic flowmeter was calibrated in the standard manner by perfusing the flow probe on the T-tube with saline at several different pressures. Volume flow rates were determined by timing the accumulation of known amounts of perfusate, and these rates were compared with the voltage output from the flowmeter. The zero-flow calibration obtained by occluding the aorta was checked at the end of each experiment by injecting acetylcholine. This drug caused the heart to slow to less than 5 beats min^{-1}. At these low heart rates the constant flow signal in the latter part of diastole was taken to represent zero flow. Dynamic calibration was not performed, but a previous study using the same flowmeter (Langille & Jones, 1977) showed that signal distortion would be negligible at the low frequencies encountered in this investigation.

Pressure and flow data were recorded on an instrumentation FM tape recorder (Hewlett-Packard 3907C) and displayed simultaneously on a strip chart recorder (Gulton Techni-rite TR888) or played back from the tape onto a Hewlett-Packard pen recorder (HP-7402A).

Determination of aortic impedance

Analogue recordings of pressure and flow pulses were digitized and signal-averaged using an analogue-to-digital converter and a Minc 11/23 computer (Digital Equipment Corp.). A sampling interval of 0·08 s allowed each pulse to be described by about 75 points. These data were then subjected to standard Fourier analysis to determine the aortic impedance spectrum (Attinger, Anne & McDonald, 1966; Gessner, 1972). Briefly, the oscillations in blood pressure and flow were represented as periodic functions by finite Fourier (harmonic) series. Thus,

$$P(t) = P_o + \sum_{n=1}^{N} P_n \cos(n\omega t - \gamma_n), \quad (1)$$

$$Q(t) = Q_o + \sum_{n=1}^{N} Q_n \cos(n\omega t - \beta_n), \quad (2)$$

where P(t) is the pressure function, Q(t) is the flow function, P_o is the mean pressure, Q_o is the mean flow, n is the harmonic number, N is the total number of harmonics, P_n and Q_n are the respective amplitudes of the nth harmonic of the pressure and flow waves, γ_n and β_n are the phase angles of each harmonic relative to

the fundamental, and ω is the angular frequency ($\omega = 2\pi f$, where f is the fundamental frequency of the heart). The mean peripheral resistance R, was calculated from the mean values of pressure and flow as:

$$R = P_o/Q_o \,. \tag{3}$$

Aortic input impedance is a complex quantity which describes the opposition to pulsatile flow in the system. Impedance amplitude Z_n and phase ϕ_n for each harmonic frequency can be expressed as (Gessner, 1972):

$$Z_n = P_n/Q_n \,, \tag{4}$$

$$\phi_n = (\beta_n - \gamma_n) \,. \tag{5}$$

In the absence of reflected waves the input impedance is equivalent to Z_o, the characteristic impedance of the tube (McDonald, 1974). Z_o is dependent upon the pressure wave propagation velocity and thus on the elasticity of the vessel wall. Z_o was calculated from (Gessner, 1972):

$$Z_o = \varrho C_o/\pi r^2 \,, \tag{6}$$

where C_o is the characteristic pressure wave velocity (see equation 11), r is the internal radius at mean blood pressure and ϱ is the fluid density (for octopus blood $\varrho \approx 1{\cdot}03\,\mathrm{g\,cm^{-3}}$). This equation describes the simple case in which viscosity of the blood and the vessel wall are neglected. Viscous effects on oscillatory flow will be dominant when the Womersley parameter, α, is less than 1 and negligible when α is greater than about 10 (Caro, Pedley, Schroter & Seed, 1978). This parameter can be calculated as $r(\varrho 2\pi f/\mu)^{\frac{1}{2}}$, where μ is the blood viscosity. For a typical animal in this study ($r = 0{\cdot}37$ cm, $\varrho = 1{\cdot}03\,\mathrm{g\,cm^{-3}}$, $f = 0{\cdot}21$ Hz, $\mu = 0{\cdot}0011$ Pa·s), $\alpha = 4{\cdot}1$. This is comparable to values of α in the aorta of small mammals such as the rabbit (McDonald, 1974). Thus, inertial forces dominate pulsatile flow in the octopus aorta, and neglecting viscosity will give only slight errors in calculations of impedance and wave velocities.

The input impedance spectrum for a Windkessel model of the octopus aorta was calculated from the electrical analogue (Fig. 1B) according to Langille & Jones (1977).

$$Z = R/[1+(2\pi fT)^2]^{\frac{1}{2}} \,, \tag{7}$$

$$\phi = -\tan^{-1}(2\pi fT) \,, \tag{8}$$

where R is the vascular resistance, f is the frequency and T is the time constant of the Windkessel. In this model, pressure decays exponentially during diastole when Q_{in}, the flow into the system, is essentially zero. The time constant T was determined experimentally from the pressure pulse profile using:

$$T = t/\ln(P_i/P_d) = RC \,, \tag{9}$$

where t is the duration of the diastole, P_i and P_d are, respectively, the initial and final diastolic pressures, and C is the capacitance or compliance of the elastic chamber.

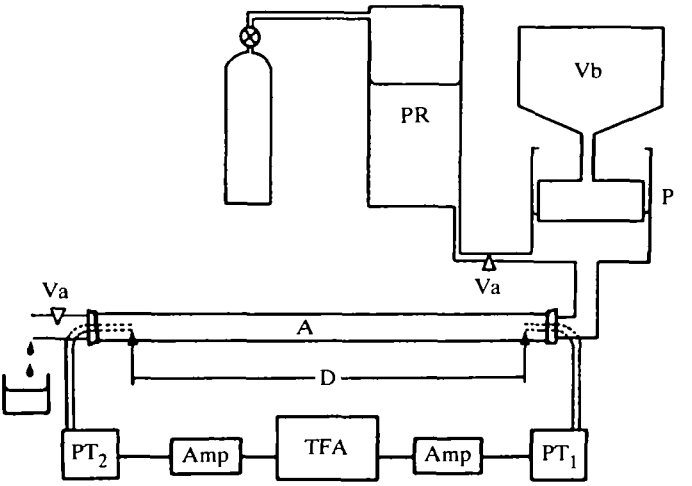

Fig. 2. A diagram of the apparatus for measuring pressure wave velocity in the aorta *in vitro*. The sample (A) is pulsed by a sinusoidal pump (P) driven by a vibrator (Vb). A steady mean pressure is maintained by a high-pressure reservoir (PR) connected across a needle valve (Va) to the pump. PT_1 and PT_2 are transducers for measuring pressure at the inflow (proximal) and outflow (distal) sites, respectively, separated by a distance D (= 15 cm). Pressure signals are processed by matched d.c. amplifiers (Amp) and compared for phase and amplitude by a Transfer Function Analyser (TFA).

Determination of pressure wave velocity

The pulse wave velocity was estimated by measuring the transit time of a pressure pulse along the aorta *in vitro*. Pressure recordings were made simultaneously at two different locations and differentiated by a Biotronix BL620 analogue computer. The resultant dP/dt signals were compared for an estimate of the transit time.

In vitro experiments were conducted to measure the velocity of sinusoidal pressure waves in the octopus aorta over a wider range of frequencies than occurs *in vivo*. An entire aorta, 16 cm long, was dissected and cannulated, with all branch vessels ligated. The specimen was inflated as shown in Fig. 2. Steady perfusion of the vessel was provided from a chamber of filtered sea water which was pressurized to 60 kPa by a compressed air source. Flow was regulated by needle valves so that a large pressure drop occurred across the inflow to the pump, while only a small pressure drop occurred at the outflow of the vessel segment. This allowed us to perfuse the artery at constant pressures of 3 and 6 kPa, while preventing the oscillatory flow from passing back into the reservoir. The diaphragm pump, driven by an electromagnetic vibrator, imposed small sinusoidal volume changes on the inflated artery such that the resulting pressure oscillations were no more than 0·3 kPa peak-to-peak, and essentially sinusoidal. Simultaneous measurements of the proximal and distal pressures were made with two identical BioTec BT-70 pressure transducers. The signals were amplified by matched d.c. amplifiers (SE Labs, Type 4200). The amplitude and phase of the two pressure waves were measured at each frequency by a Transfer Function Analyser (SE Labs, type SM272DP; see Denny & Gosline,

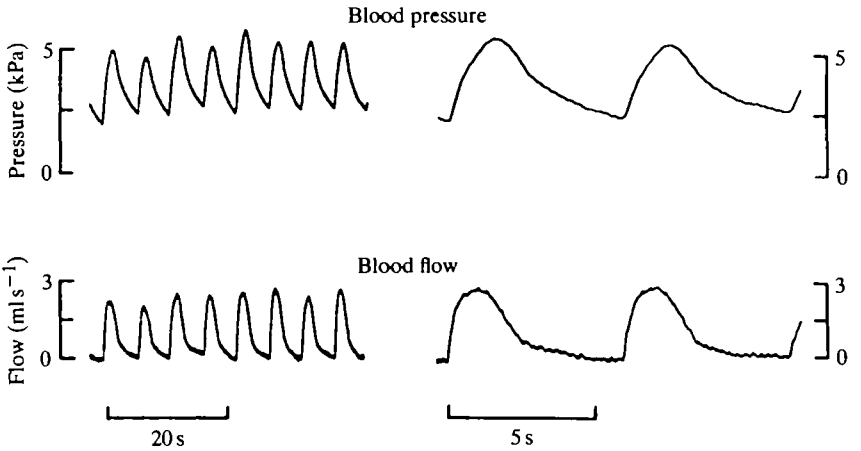

Fig. 3. Analogue pressure and flow, recorded in the aorta of a resting octopus.

1980). Pressure transducers were calibrated as described above. The apparent pulse wave velocity (C′) was computed for each frequency from:

$$C' = 2\pi fD/\theta\,, \tag{10}$$

where θ is the phase difference in radians between proximal and distal pressures measured at sites that are separated by a distance D. The transmission ratio was determined as the ratio of distal to proximal pressure amplitudes. In the absence of reflections, the velocity of pressure waves in the aorta is the characteristic or intrinsic wave velocity C_o. This was calculated for a thick-walled viscoelastic tube, according to Saito & VanderWerf (1975):

$$C_o = (2E'h/3\varrho r)^{\frac{1}{2}}\,, \tag{11}$$

where E′ is the dynamic elastic (storage) modulus of the wall in the circumferential direction, and h is the vessel wall thickness.

RESULTS

Aortic blood pressure and flow in the resting octopus

Systemic heart rates in resting octopuses at 8–10°C ranged from 8·5 to 14 beats min^{-1} (0·14–0·23 Hz). Aortic blood pressure varied from 2·1 to 2·9 kPa at end diastole, and from 3·6 to 6·1 kPa at peak systole. During periods of spontaneous exercise, blood pressure increased to as high as 4·5 kPa at end diastole and 8 kPa at peak systole. Blood flow was pulsatile and varied with pressure, with the mean value averaging 0·9 ml s^{-1}. Peak flows ranged from 1·4 to 2·8 ml s^{-1}, which, when averaged across the vessel cross-section, correspond to peak velocities of 0·03–0·06 m s^{-1}. Examples of stroke volume and cardiac output calculated from these data are 5·4 ml and 5·4 ml min^{-1} kg^{-1}, respectively (for a 10-kg octopus with a heart rate of 10 beats min^{-1}).

Typical analogue pressure and flow records are shown in Fig. 3. Digitized, signal-averaged data are plotted in Fig. 4. The shape of these waveforms indicates that a

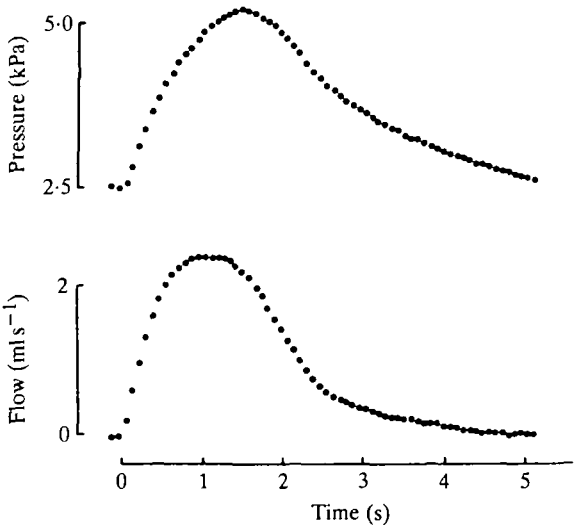

Fig. 4. Digitized, signal-averaged pressure and flow waves from the data of Fig. 3.

central elastic reservoir is present. Systolic ejection began with a rapid rise in both the pressure and the flow velocity. Peak flow was reached after about 1 s, while peak pressure was attained some 0·6 s later. The end of systole was not marked by an incisura in the pressure wave or by flow reversal, as it is in mammals. Presumably, closure of the aortic valves and the beginning of diastole occurred at about the inflection point in the decreasing flow curve, which came about 1·5 s after its peak value. Both flow and pressure continued to decrease asymptotically towards their end diastolic values, which for flow was approximately zero.

Aortic impedance spectra

The amplitudes of the major harmonics of the pressure and flow waves of Fig. 4 are shown in Fig. 5. The zero harmonics give the mean values of pressure and flow (P_o and Q_o), which in this case were 3·9 kPa and 0·85 ml s^{-1}, respectively. The first harmonic occurs at the fundamental frequency of the heart beat, while subsequent harmonics occur at integer multiples of this frequency. As one might expect from the fairly smooth shape of the pressure and flow curves, the higher frequencies are relatively unimportant. The amplitudes of harmonics above the fifth were less than 5 % of the amplitude of the fundamental. In addition, over 99 % of the pulsatile hydraulic power, as computed from pressure and flow curves (Gessner, 1972), was delivered in the first five harmonics. Thus the pressure and flow pulses in the octopus aorta can be closely approximated by Fourier series of five harmonics.

Aortic impedance spectra are shown in Fig. 6. For comparisons among individuals, Z is normalized with respect to the impedance at zero frequency, i.e. the mean resistance R. This emphasizes the difference between the impedance to steady *versus* pulsatile flow. In each animal, impedance amplitude decreased sharply to approximately 20 % of R at the first harmonic. At frequencies above the fundamental, the impedance displayed a general but much more gradual decline to around

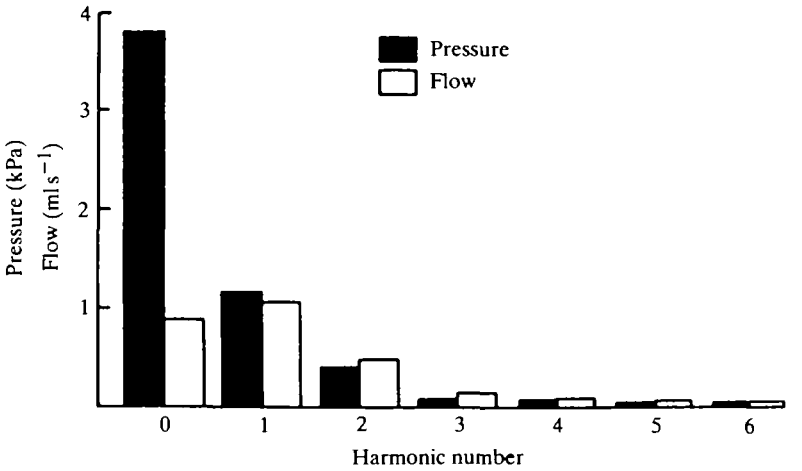

Fig. 5. The amplitudes of the first six harmonics of pressure and flow waves from Fig. 4. The mean value of each function is the zero harmonic. The first harmonic occurs at the fundamental frequency, which is 0·18 Hz in this example.

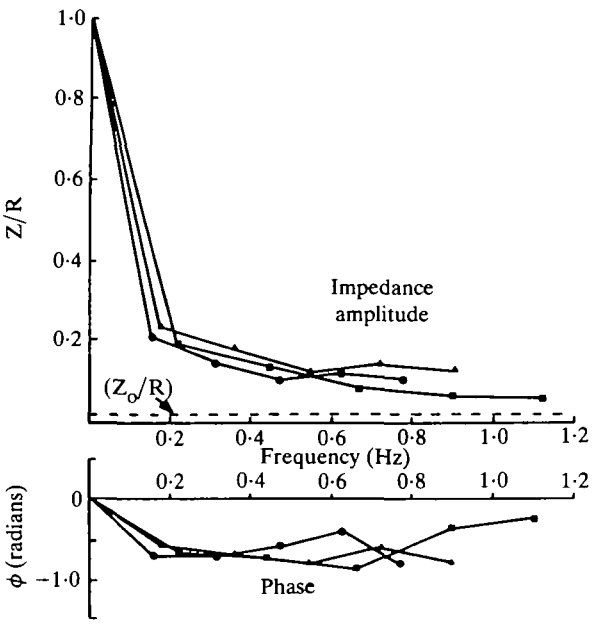

Fig. 6. Aortic impedance spectra for three octupuses. Data for the first five harmonics are shown, and represent 150 signal-averaged pulses of pressure and flow. Impedance amplitude, Z, is expressed as a proportion of the mean resistance, R, as is the characteristic impedance, Z_o (broken line). The actual values of R in these experiments were 5·65, 4·50 and $7{\cdot}77 \times 10^9$ Pa·s m^{-3}, while Z_o/R ranged from 0·023 to 0·028. Negative phase angles indicate that flow leads pressure.

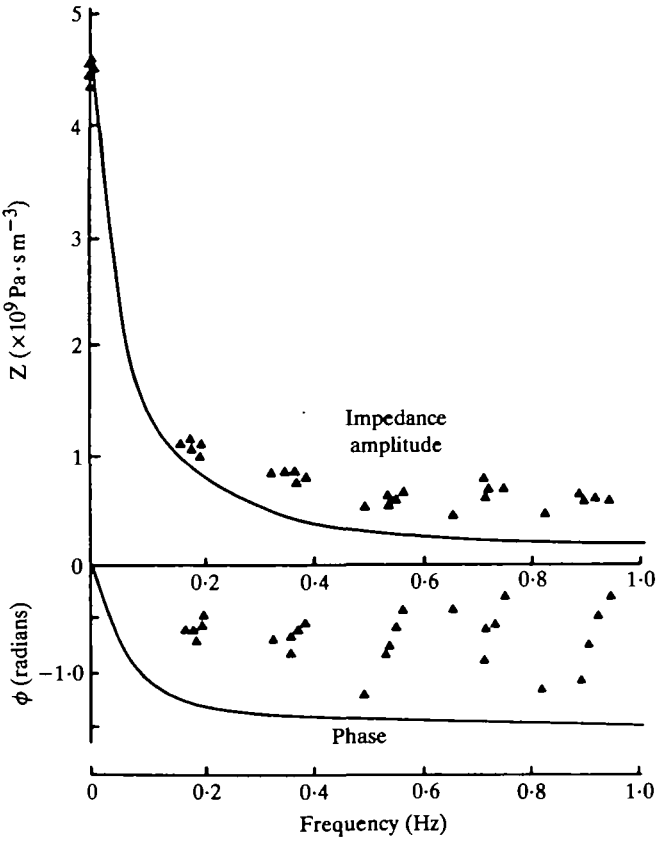

Fig. 7. Impedance amplitude and phase for one octopus, compared to model curves predicted from the Windkessel model (equations 7, 8).

10 % of R. The characteristic impedance, Z_o, was calculated for each aorta (equation 6). The average value of Z_o/R was 0·026, and this is indicated by the dashed line in Fig. 6. Impedance phase was always negative (flow leading pressure), decreasing to about −0·65 radians at the first harmonic, and fluctuating around this value at higher harmonics.

In Fig. 7, impedance data are plotted for one octopus, along with amplitude and phase curves predicted for that animal from the electrical analogue of the Windkessel model (equations 7, 8). This simple two-element model gave a reasonable approximation of the impedance data, particularly at the lower frequencies, although the predicted values of amplitude and phase were consistently lower than those observed.

Pressure wave propagation in the aorta

Estimates of intrinsic pressure wave velocity, C_o, were obtained from equation 11, using values of the dynamic elastic modulus of the aortic wall (Shadwick & Gosline, 1985). Table 1 shows that C_o was highly dependent on pressure, and to a lesser degree on frequency, due to the non-linear elastic properties of the aorta. In a 10-kg

Table 1. *Predicted intrinsic pressure wave velocity, C_o, and wavelength, λ, for two mean pressures*

Pressure		Frequency (Hz) 0·1	0·5	1·0	5·0	10·0
3 kPa	C_o ($m\,s^{-1}$)	2·17	2·31	2·34	2·46	2·54
	λ (m)	21·7	4·62	2·34	0·49	0·25
6 kPa	C_o ($m\,s^{-1}$)	5·98	6·28	6·68	7·95	8·18
	λ (m)	59·8	12·56	6·68	1·59	0·82

C_o is calculated from equation 11, and λ is calculated from $C_o = f\lambda$, where f is frequency.

octopus, L (the length of the aorta from the heart to the region of arborization in the head) was about 15 cm. For such an animal, with a mean blood pressure of 3 kPa, a pressure pulse at 0·2 Hz should travel at about 2·25 $m\,s^{-1}$, and the transit time through the aorta would be about 70 ms. At a mean pressure of 6 kPa the velocity would be just over 6 $m\,s^{-1}$, and the pulse would reach the periphery in only 25 ms. Thus, transmission of pressure waves through the aorta of a resting octopus should normally take a negligible portion (0·4–1·6 %) or a cardiac cycle. Table 1 also gives wavelengths calculated for each frequency and pressure. Note that within the physiological range of frequencies (up to 1 Hz) λ was very large relative to L. Only at frequencies above 5 Hz did the length of the aorta represent an appreciable fraction of the pressure wavelength.

Fig. 8 shows a typical example of a pressure wave in the octopus aorta which was recorded simultaneously at two sites 10 cm apart. The fundamental frequency was 0·14 Hz and the mean pressure was approximately 3 kPa. The pressure pulse was transmitted through the aorta with only slight attenuation and virtually no change in the shape of the waveform, in contrast to the distortion and peripheral amplification of the pressure pulse which occurs in mammals (McDonald, 1974). Measurements of pressure wave velocity were difficult to make *in vivo*. In all instances, the pulses appeared at both recording sites in virtual synchrony. Normally the wave velocity is determined from the transit time of the foot of the wave over a given distance. From our calculations of C_o (Table 1) this should have been about 50 ms, but no actual time difference could be discerned between the two recordings. Differentiated pressure waves had a more sharply defined foot, and a distinct peak (Fig. 8B). By comparing these waveforms the transit time was determined to be less than 10 ms. Thus the apparent wave velocity C′ was in excess of 10 $m\,s^{-1}$, or more than four times greater than C_o, as predicted from the mechanical properties of the artery wall.

To test predictions of intrinsic wave velocity, we studied the propagation of pressure pulses in the octopus aorta at higher frequencies (i.e. shorter wavelengths) than normally occur in the animal. Fig. 9A shows the results of *in vitro* experiments in which small sinusoidal pressure waves were generated in an aorta which was being perfused at a mean pressure of 3 kPa. The apparent wave velocity, C′ was highly frequency-dependent. Values of C′ fell sharply from about 30 $m\,s^{-1}$ at 1 Hz to a minimum of 2·30 $m\,s^{-1}$ at 6 Hz, and thereafter rose slightly to 2·90 $m\,s^{-1}$ at 10 Hz. Recall that C_o was approximately 2·50 $m\,s^{-1}$ at 5–10 Hz (Table 1), while *in vivo* C′

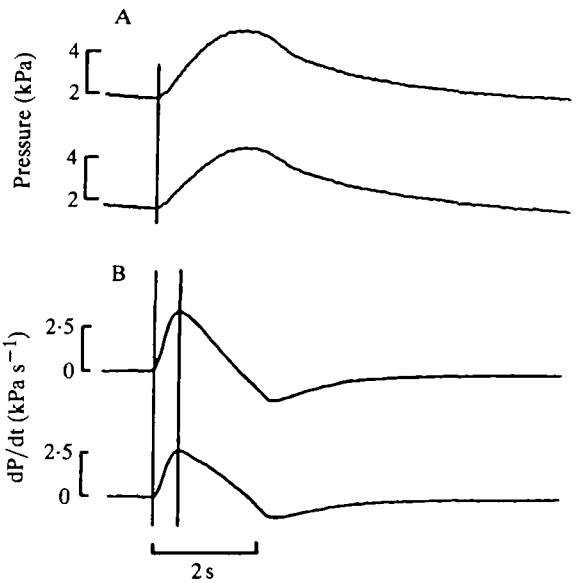

Fig. 8. (A) A pressure pulse in the octopus aorta measured simultaneously at two points separated by 10 cm (upper trace is from the proximal site; lower trace is from the distal site). The waves are in virtual synchrony. (B) The differentiated pressure pulses of A. These wave-forms have a more distinct 'foot' than the originals. Time differences between pairs of differentiated pressure waves were determined to be less than 10 ms, which indicates an apparent wave velocity of greater than 10 m s^{-1}.

was in excess of 10 m s^{-1} at frequencies below 1 Hz. Thus, the data in Fig. 9A are consistent with the *in vivo* measurements at low frequencies, and with the predictions of intrinsic velocity at high frequencies. These results suggest that pressure waves at frequencies above 6 Hz were propagated with little influence from terminally reflected waves, while below this frequency reflections became increasingly important and gave rise to very high apparent velocities. The transmission ratio increased from 1·0 to a maximum value at about 5 Hz, then decreased towards 1·0 again at higher frequencies. This means that the pressure waves were amplified distally due to positive or 'closed-end' type reflections, caused by the increased impedance at the distal cannula. A partial resonance occurred in the test specimen at approximately the same frequency where C′ reached its minimum. Pressure waves should be attenuated because of viscous energy losses, primarily arising in the artery wall viscosity (McDonald, 1974; Caro *et al.* 1978). We calculated the transmission ratio of pressure waves without reflections according to Taylor (1966*a*) and, as shown in Fig. 9 (broken lines), this decreased from 1·0 with increasing frequency.

When the aorta was tested at a mean pressure of 6 kPa, we found that with increasing frequency the apparent velocity fell from initial values near 100 m s^{-1} to below 10 m s^{-1} at 15 Hz, while the transmission ratio rose continuously from 1·0 (Fig. 9B). Data for the storage modulus, E′, used to predict C_o, were available only up to 10 Hz. At this frequency C_o was 8·18 m s^{-1} (Table 1), well below the apparent velocity C′. The range of frequencies was not great enough to reveal a minimum in

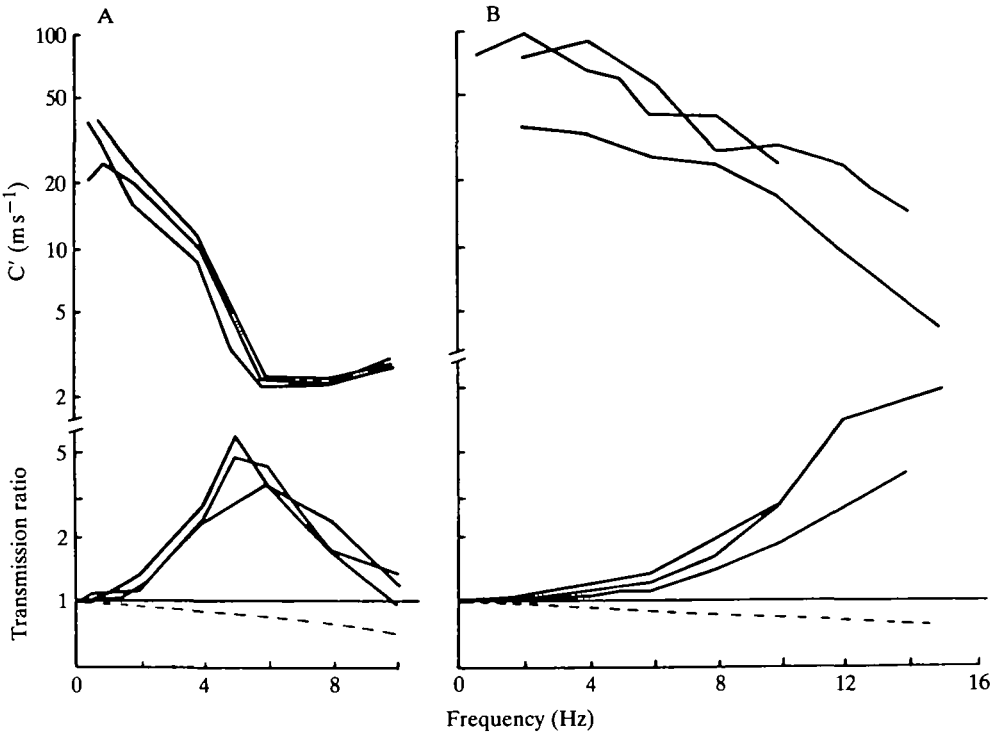

Fig. 9. Apparent wave velocity (C′, upper curves) and transmission ratios (lower curves) *versus* frequency, measured in an aorta *in vitro* at mean pressures of 3 kPa (A), and 6 kPa (B). The broken lines show the expected transmission ratio, in the absence of reflected waves, due to viscous energy losses from the artery wall viscosity.

the C′ curve, nor a maximum in the transmission ratio, as were seen at the lower pressure (Fig. 9A). Extrapolation of the E′ data, however, yields an estimate of C_o of $8{\cdot}4\,m\,s^{-1}$ at 15 Hz, and this is approximately equal to the measured values of C′ at this frequency. Thus the frequency of resonance at 6 kPa may occur at close to 15 Hz.

DISCUSSION

Pressure and flow waveforms

Simultaneous recordings of blood pressure and flow pulses are presented for the first time in a cephalopod mollusc. The data provide direct evidence that the dorsal aorta in *Octopus dofleini* functions as a central elastic reservoir or Windkessel. The octopus blood pressure pulse followed a smooth and near-exponential decay in diastole, with no indication of any secondary peaks or alterations in the pressure profile as the wave travelled peripherally. Blood pressure waveforms obtained in this study are similar to records obtained previously from *O. dofleini* (Johansen & Martin, 1962) and from other cephalopods (Bourne, Redmond & Johansen, 1978; Wells, 1979; Bourne, 1982). Our estimate of stroke volume and cardiac output in *O. dofleini* is 10–30 % lower than those determined by Johansen (1965) using the Fick method. This difference is probably because, in our experiments, some of the ventricular

outflow passed through vessels to the viscera and mantle rather than through the flow probe on the dorsal aorta. Johansen & Martin (1962) suggested that the lack of incisura in the octopus aortic pressure pulse was due to some functional anatomical difference between the aortic valves of cephalopods and vertebrates. While this is possible, the position of the recording site which was several centimetres from the heart, and therefore peripheral to a substantial portion of the elastic reservoir provided by the aorta, would contribute to the disappearance of an incisura and concomitant flow reversal which may well occur immediately adjacent to the heart. The same phenomenon is seen in flow pulses recorded from the pulmonary arteries of turtles (Shelton & Burggren, 1976) and the ventral aorta of fish (Jones, Langille, Randall & Shelton, 1974).

The importance of the location of the flow probe on the aorta is demonstrated in Fig. 10, where we calculate the flows in a simple Windkessel model of the octopus circulation. Outflow through the peripheral resistance, Q_r, is relatively steady and is proportional to the pressure. However, the calculated flow into the system, Q_{in}, (i.e. the ventricular outflow) is highly pulsatile and is proportional to the rate of change of pressure. The change in shape of the flow pulse as it passes through the Windkessel involves a reduction of the pulse amplitude and a phase shift of almost a quarter cycle. The actual flow pulse, Q(t), which was measured partway along the aorta, has partially undergone this transformation. The sustained diastolic flow seen in Q(t) must be supplied by elastic recoil in the upstream portion of the highly compliant aorta. Note that the predicted Q_{in} is similar in shape to the flow pulse in the ascending aorta of mammals, in which there is an incisura coincident with flow reversal (McDonald, 1974). In the octopus aorta, the measured pressure pulse containing no incisura is not inconsistent with a ventricular outflow pattern that has a distinct period of reversal at the end of systole. Thus, it is not necessary to postulate that the aortic valves in this cephalopod are functionally different from those in vertebrates.

Impedance spectra

The impedance spectrum we determined for the octopus aorta is substantially different from that which is typically observed in mammals (McDonald, 1974). Oscillations in impedance amplitude and phase, which characterize a transmission-line system like the mammalian aorta, are not evident in the octopus aortic impedance curves. Instead, impedance amplitude declines continuously with increasing frequency, but remains 3–5 times greater than Z_o after the fifth harmonic, while impedance phase remains relatively constant and negative (Fig. 7). In constrast, in mammals such as rabbits, dogs and man, impedance amplitude decreases sharply and oscillates about the level of Z_o after the first harmonic (O'Rourke & Taylor, 1967; McDonald, 1974). Since Z_o defines the pressure:flow ratio in the complete absence of reflected waves, the mammalian aorta approximates a reflection-free system for harmonics above the fundamental frequency (Taylor, 1964, 1966*a*), while the octopus aorta is dominated by reflections at all harmonic

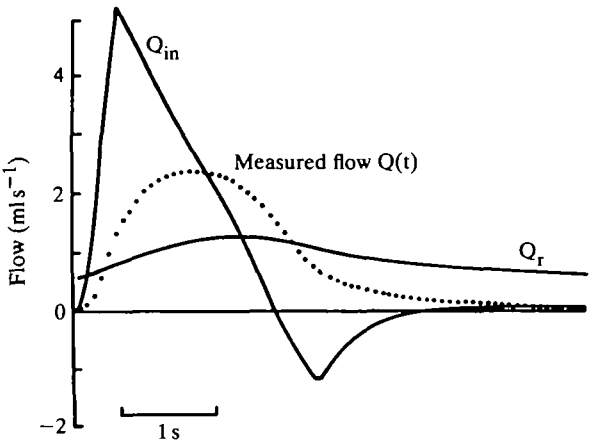

Fig. 10. Components of flow through the Windkessel model (see Fig. 1), predicted from the averaged *in vivo* pressure pulse of Fig. 4. Q_r is the outflow across the resistor and is directly proportional to pressure, P. Q_{in} is the inflow to the system, and is equal to $C(dP/dt) + (P/R)$, where $C = T/R$ (equation 9), $P/R = Q_r$. Q(t) is the *in vivo* flow pulse measured simultaneously with the pressure. In this example $P_o = 3{\cdot}95$ kPa, $Q_o = 0{\cdot}885$ ml s^{-1}, $R = 4{\cdot}37\times10^9$ Pa·s m^{-3}, $T = 5{\cdot}99$ s and $C = 1{\cdot}37\times10^{-9}$ m^3·Pa^{-1}.

frequencies. Consequently, the octopus aorta acts much more like a simple Windkessel rather than a complex transmission line.

The discrepancy between the measured aortic impedance spectra and the Windkessel predictions (Fig. 7) is probably because the flow probe was not placed immediately adjacent to the heart. Therefore, the data in Figs 6 and 7 do not represent the input impedance of the entire aortic Windkessel (as do the model curves) but describe the local fluid impedance; i.e. the input impedance of that portion of the arterial circulation which was distal to the probe. The local impedance must be altered as the point of reference is moved along the aorta, because the pulsatile inflow from the heart is transformed to a much smoother flow by the compliance of the vessel wall. Fig. 10 indicates that towards the periphery impedance phase would become less negative and impedance amplitude would increase. If pressure and flow were measured at the very end of the Windkessel, impedance amplitude would equal R and phase would be zero. In mammals such changes are seen in the aortic impedance as the recording sites are moved peripherally (McDonald, 1974).

There are other factors which can contribute to differences between our impedance data and the model predictions. The octopus aorta has non-linear elastic properties, so the compliance is not a constant but varies over the pressure pulse (Shadwick & Gosline, 1985). Thus, the diastolic pressure decay is not a simple exponential, so the value T is only an approximation of a spectrum of time constants for the system. In addition, the model lumps all resistance as a single peripheral element. The octopus aorta is modelled as a capacitor, but it must also represent a resistor because it is a tube with finite dimensions. In reality, there must be some resistance to flow in the aorta, although Z_o is only about 3 % of R. According to

Westerhof, Elzinga & Sipkema (1971), the addition of Z_o to the model increases the impedance amplitude and makes the phase less negative.

Reflection effects on wave velocity and impedance

The fundamental feature of the octopus circulation which allows the system to be inflated by the heart as a single elastic reservoir, rather than as a complex transmission line, is that the major harmonic components of the pressure pulse have wavelengths which are very long compared to the aorta (Table 1). The combination of these waves with strong reflections yields a pressure pulse which appears to travel at very high velocity. Thus, the apparent wave velocity *in vivo*, C′, was much greater than the intrinsic wave velocity, C_o. Similarly, the deviation in Z from the characteristic value, Z_o, is due to the presence of reflected waves in the system (McDonald, 1974; Noordergraaf, 1978). Reflections are generated in the arterial tree by changes in impedance, the predominant source being major branch sites. During a continuous train of pressure pulses, the interaction of incident and reflected waves produces oscillations in amplitude along the aorta as well as oscillations in the phase, and therefore the apparent velocity, of the resultant wave (Taylor, 1957; Caro & McDonald, 1961; McDonald, 1974). For each sinusoidal component of the pulse, nodes and antinodes occur alternately at quarter-wavelength intervals along the length of the aorta. Since pressure waves are attenuated due to viscosity, the oscillations in pressure amplitude and apparent velocity become more damped as the distance, in wavelengths, between the reflection site and the point of observation is increased (Taylor, 1966*b*; McDonald, 1974). Thus, at high frequencies and short wavelengths, the apparent velocity in the aorta will approximate the reflection-free value, C_o, as in our *in vitro* experiments (Fig. 9).

Clearly, wavelength is the critical parameter in the analysis of pressure wave velocity in a viscoelastic tube of finite length. In Fig. 11 the measurements of C′ are summarized, along with the predicted curves for C_o at pressures of 3 and 6 kPa. The frequency scale is given in terms of wavelengths; specifically, the ratio L/λ is plotted, where L is the tube length and λ is the wavelength. Frequency and wavelength are inversely related, so that with increasing frequency L becomes a larger proportion of λ. The first minimum in C′ should occur at the frequency where $L/\lambda = 0{\cdot}25$ (McDonald, 1974). At a pressure of 3 kPa L was 12 cm. Fig. 11 shows that the quarter-wavelength frequency, predicted from C_o, was 5·2 Hz. The observed quarter-wavelength frequency fell between 5 and 6 Hz, as indicated by the minimum in C′ and the maximum in transmission ratio (Figs 9A, 11). Transmission ratio peaks at the nodal frequency because the upstream pressure is at its minimum and the downstream pressure is at its maximum, a condition described as a partial resonance (Taylor, 1966*a*). The good agreement between predicted and observed quarter-wavelength frequency for the aorta verifies our measurement of the vessel elasticity. Above this frequency the data indicate that oscillations in C′ will be highly damped. At 10 Hz (about the half-wavelength frequency) C′ was only slightly greater than C_o. In the octopus, the physiological range is well below the quarter-wavelength frequency ($L/\lambda < 0{\cdot}05$), and consequently C′ rises to anomalously high values.

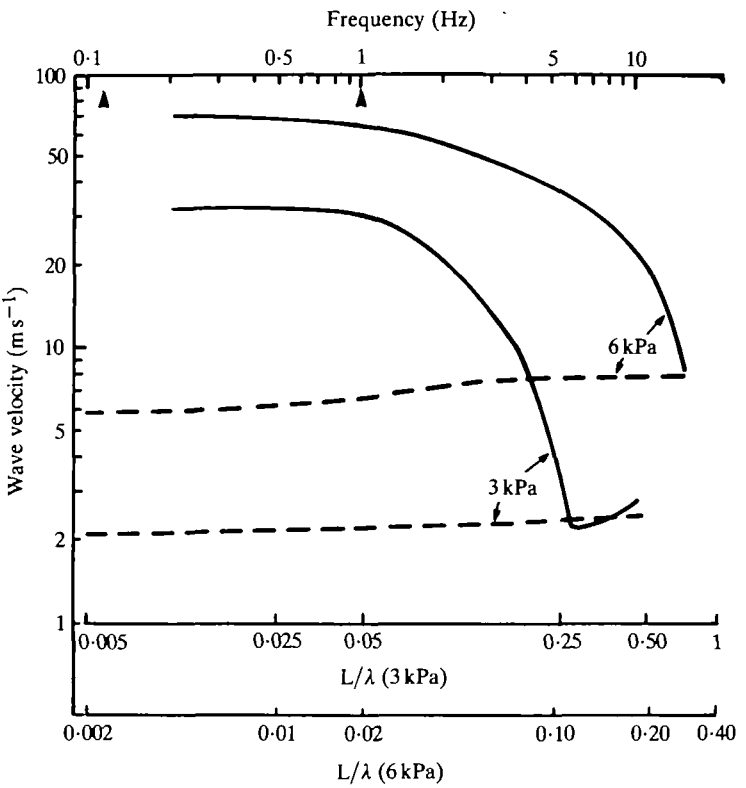

Fig. 11. Apparent wave velocity curves (solid lines) from the data of Fig. 9, plotted with the predicted characteristic velocity, C_o, (broken lines) for pressures of 3 and 6 kPa. Frequency scale (upper abcissa) has been transformed into the relative wavelength, based on C_o, for each pressure (lower abcissae). Arrows indicate the frequency range of harmonics of the *in vivo* pressure pulse.

Results of tests at 6 kPa can be interpreted as showing the same behaviour as was seen at 3 kPa if frequency is expressed as the ratio L/λ. Since C_o increases with pressure, all wavelengths increase. The quarter-wavelength frequency is extended to about 15 Hz, and L/λ for the physiological range is $<0{\cdot}02$.

These results can be applied to the *in vivo* circulation, if we consider that the length of the test specimen was about 80 % of the entire aorta, and the preparation was perfused with sea water, which is slightly less viscous than octopus blood. Increasing the tube length and the fluid viscosity will tend to reduce the nodal frequency and transmission ratios somewhat (Taylor, 1966*a*,*b*). We estimate that for a mean pressure of 3 kPa *in vivo* the minimum in C′ would occur at about 4 Hz. The physiologically significant harmonic components of the pressure pulse will have wavelengths 10–200 times longer than the entire aorta. This means the heart is separated from the major peripheral branch sites by a distance which is less than 1 % of the wavelength of its fundamental frequency. Over this short distance wave reflection anomalies give apparent wave velocities 15–20 times higher than the true

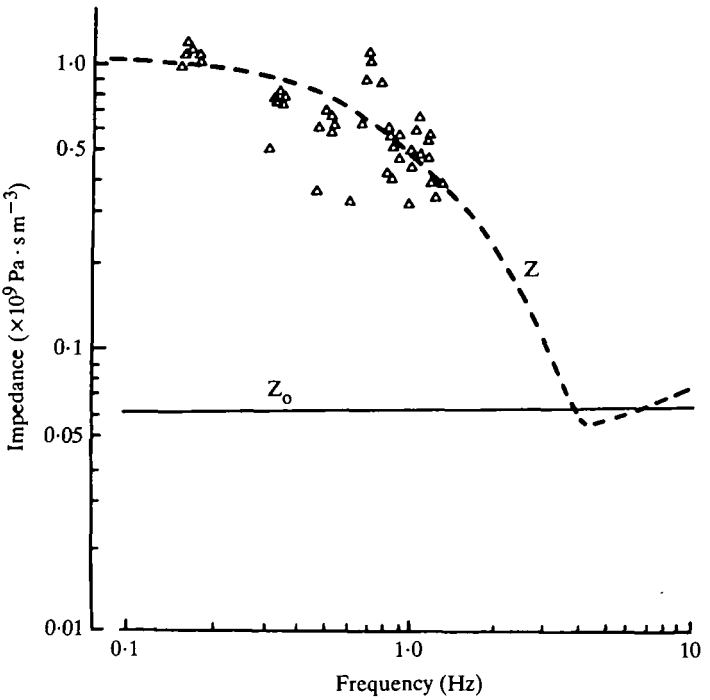

Fig. 12. Calculated impedance amplitude (Z, broken line), based on the data for C′ in Fig. 11, for a pressure of 3 kPa. Z_o (solid line) is predicted from C_o (equation 6). Data points are measured values of Z from an octopus in which the mean pressure was 3 kPa.

wave velocity. Thus, in the octopus, the aorta will indeed be inflated in virtual synchrony throughout, as a single elastic reservoir.

Due to reflections and viscosity the input impedance of a viscoelastic tube shows a pattern of decreasing oscillations with increasing frequency which parallels the oscillations of pressure amplitude and apparent velocity in a transmission line (McDonald, 1974). So, impedance amplitude will be high at very low frequencies, fall to a minimum at the quarter-wavelength frequency, and settle to approximately Z_o at high frequencies. Just as Z_o is directly proportional to C_o (equation 6), impedance amplitude may be calculated from C′ by a similar relationship (McDonald, 1974). Fig. 12 shows an impedance curve for the octopus aorta predicted from apparent velocity *in vitro* at 3 kPa, and shifted so that the quarter-wavelength frequency falls at the estimated *in vivo* value of 4 Hz. The impedance data from one octopus, in which mean pressure was 3 kPa, show reasonable agreement with the predicted impedance curve at the low frequencies where *in vivo* data are available.

Major differences between Windkessel and transmission-line models arise because in the former the range of frequencies occurring, or more specifically the range of L/λ, is much lower than in the latter. Thus the Windkessel may be regarded as a special case of transmission line (Noordergraaf, 1978). Fig. 12 illustrates an inherent disadvantage of the Windkessel. Since the heart rate is well below the quarter-

wavelength frequency, the impedance to pulsatile flow is always well above the level which could be experienced by the heart if frequencies were much higher. In mammals, due to the higher heart rates, the heart is functionally 'uncoupled' from the high peripheral resistance at harmonics above the second (O'Rourke & Taylor, 1967; Milnor, 1982). At these frequencies the mammalian heart works against an input impedance which approximates that of a reflection-free system, and the total pulsatile work is reduced (Taylor, 1964; Noordergraaf *et al.* 1979). Our *in vitro* experiments indicate that for the octopus a similar uncoupling of the heart from the peripheral resistance would require at least a 10-fold increase in the cardiac frequency. It seems unlikely that the increased energy cost associated with such an elevated heart rate would be outweighed by the saving from reduced impedance. In more active cephalopods, such as large pelagic squids, which have higher heart rates or longer arterial trees than *O. dofleini*, the circulatory systems may well be optimized to take advantage of wave transmission effects and reduce the work of the heart, as in mammals.

This work was supported by grants from NSERC of Canada. We are grateful to Dr David R. Jones for critical advice and the use of laboratory facilities.

REFERENCES

ATTINGER, E. O., ANNE, A., MCDONALD, D. A. (1966). Use of Fourier series for the analysis of biological systems. *Biophys. J.* **6**, 291–304.

BOURNE, G. B. (1982). Blood pressure in the squid *Loligo pealei*. *Comp. Biochem. Physiol.* **72A**, 23–27.

BOURNE, G. B., REDMOND, J. R. & JOHANSEN, K. (1978). Some aspects of hemodynamics in *Nautilus pompilius*. *J. exp. Zool.* **205**, 63–70.

BURGGREN, W. (1977). The pulmonary circulation of the chelonian reptile: morphology, hemodynamics and pharmacology. *J. comp. Physiol.* **116**, 303–323.

CARO, C. G. & MCDONALD, D. A. (1961). The relation of pulsatile pressure and flow in the pulmonary vascular bed. *J. Physiol., Lond.* **157**, 426–453.

CARO, C. G., PEDLEY, T. J., SCHROTER, R. C. & SEED, W. A. (1978). *The Mechanics of the Circulation*. Oxford: Oxford University Press.

DENNY, M. W. & GOSLINE, J. M. (1980). The physical properties of the pedal mucus of the terrestrial slug *Ariolimax columbianus*. *J. exp. Biol.* **88**, 375–394.

GESSNER, U. (1972). Vascular input impedance. In *Cardiovascular Fluid Dynamics*, vol. I (ed. D. H. Bergel), pp. 315–349. New York: Academic Press.

JOHANSEN, K. (1965). Cardiac output in the large cephalopod *Octopus dofleini*. *J. exp. Biol.* **42**, 475–480.

JOHANSEN, K. & MARTIN, A. W. (1962). Circulation in the cephalopod *Octopus dofleini*. *Comp. Biochem. Physiol.* **5**, 161–176.

JONES, D. R., LANGILLE, B. L., RANDALL, D. J. & SHELTON, G. (1974). Blood flow in dorsal and ventral aortas of the cod, *Gadus morhua*. *Am. J. Physiol.* **226**, 90–95.

LANGILLE, B. L. & JONES, D. R. (1977). Dynamics of blood flow through the hearts and arterial systems of anuran amphibia. *J. exp. Biol.* **68**, 1–17.

MCDONALD, D. A. (1974). *Blood Flow in Arteries*. London: Edward Arnold.

MILNOR, W. R. (1982). *Hemodynamics*. Baltimore, London: Williams & Wilkins.

NOORDERGRAAF, A. (1978). *Circulatory System Dynamics*. New York: Academic Press.

NOORDERGRAAF, A., LI, J. K.-J. & CAMPBELL, K. B. (1979). Mammalian hemodynamics: a new similarity principle. *J. theor. Biol.* **79**, 485–489.

O'ROURKE, M. F. & TAYLOR, M. G. (1967). Input impedance of the systemic circulation. *Circulation Res.* **20**, 365–380.

PACKARD, A. (1972). Convergent evolution between cephalopods and vertebrates. *Biol. Rev.* **47**, 241–307.

SAITO, G. E. & VANDERWERFF, T. J. (1975). The importance of viscoelasticity in arterial blood flow models. *J. Biomech.* **8**, 237–245.

SHADWICK, R. E. & GOSLINE, J. M. (1985). Mechanical properties of the octopus aorta. *J. exp. Biol.* **114**, 259–284.

SHELTON, G. & BURGGREN, W. (1976). Cardiovascular dynamics of the chelonia during apnoea and lung ventilation. *J. exp. Biol.* **64**, 323–343.

TAYLOR, M. G. (1957). An approach to the analysis of the arterial pulse wave. II. Fluid oscillations in an elastic tube. *Physics Med. Biol.* **1**, 321–329.

TAYLOR, M. G. (1964). Wave travel in arteries and the design of the cardiovascular system. In *Pulsatile Blood Flow* (ed. E. O. Attinger), pp. 343–367. New York: McGraw Hill.

TAYLOR, M. G. (1965). Wave-travel in a non-uniform transmission line in relation to pulses in arteries. *Physics Med. Biol.* **10**, 539–550.

TAYLOR, M. G. (1966*a*). The input impedance of an assembly of randomly branching elastic tubes. *Biophys. J.* **6**, 29–51.

TAYLOR, M. G. (1966*b*). Wave transmission through an assembly of randomly branching elastic tubes. *Biophys. J.* **6**, 697–716.

WELLS, M. J. (1979). The heartbeat of *Octopus vulgaris*. *J. exp. Biol.* **78**, 87–104.

WELLS, M. J. (1983). Circulation in cephalopods. In *The Mollusca: Physiology*, Part 2, vol. 5 (ed. A. S. M. Saleuddin & K. Wilbur), pp. 239–290. New York: Academic Press.

WESTERHOF, N., ELZINGA, G. & SIPKEMA, P. (1971). Artificial arterial system for pumping hearts. *J. appl. Physiol.* **31**, 776–781.